Wood Physics/Mechanical Properties

Yuka Miyoshi*, Hisashi Abe, Hiroaki Horiyama, Keisuke Kojiro and Yuzo Furuta

Influence of habitat, density, lignin structure, and extraction treatment on thermal-softening properties of water-swollen wood: a study of 87 wood specimens

https://doi.org/10.1515/hf-2023-0083
Received August 9, 2023; accepted December 12, 2023;
published online January 15, 2024

Abstract: This study aims to reveal the diversity of thermal-softening temperatures and identify the factors that determine this temperature. To achieve this, the thermal-softening properties of the radial direction of wood were measured under water-saturated conditions for 15 softwood and 72 hardwood specimens. Wood samples were obtained from the xylarium of the Forestry and Forest Products Research Institute, Japan. A dynamic viscoelastic measurement was performed on samples with uniform heating and cooling history because the difference in cooling rate can alter in the mechanical properties of wood. The storage and loss elastic moduli increased linearly as wood density increased, regardless of the wood species. However, the thermal-softening temperature (defined in this study as the peak temperature of loss tangent) was unrelated to the density, anatomical features, species, latitude, and annual rainfall in the habitat. When the relationship between thermal-softening temperature and lignin structure was investigated, a negative correlation was observed between the thermal-softening temperature and the syringyl ratio (syringyl/(syringyl+guaiacyl)) of lignin aromatics. This indicates that the thermal-softening temperature is higher for wood species with denser lignin structures, supporting the prior research showed correlation between thermal-softening temperature and methoxyl group content of wood.

Keywords: viscoelasticity; lignin structure; density; extraction; habitat

1 Introduction

Many studies have been conducted on the thermal-softening properties of wood in the lateral direction. One study found that the peak temperature of the logarithmic decrement, measured by the torsional dynamic viscoelasticity of the radial sample, becomes lower at a higher moisture content and reaches around 80 °C when the moisture content is 20 % or more (Becker and Noack 1968). Although the thermal-softening temperature varies with the frequency of measurement and the loading direction of the sample, it is recognized that the softening behavior observed around 80 °C for the water-saturated wood is based on the glass transition of lignin (Salmén 1984). It is known that the thermal-softening temperature of water-saturated wood is higher in softwood than in hardwood (Placet et al. 2007). The lignin structure differs between softwood and hardwood because softwood contains only the guaiacyl nucleus and hardwood contains both guaiacyl and syringyl nuclei. To investigate the effect of lignin on the thermal-softening properties of various species of wood in water-saturated condition, Furuta et al. (2001, 2008a, b) measured the peak temperatures of the loss tangent (tan δ), as the thermal-softening temperature, by dynamic mechanical analysis, and compared this temperature for water-saturated wood samples (10 softwood and 12 hardwood) in the radial direction. The results showed that the thermal-softening temperature is higher for softwood species, with a difference of up to 30 °C. The authors proposed that the difference in thermal-softening temperature between tropical hardwood and Japanese hardwood is caused by a variation in the lignin structure owing to the aromatic nuclei of lignin; however, it

***Corresponding author: Yuka Miyoshi**, Department of Wood Properties and Processing, Forestry and Forest Products Research Institute, Matsunosato 1, Tsukuba, Ibaraki 305-8687, Japan, E-mail: ymiyoshi@ffpri.affrc.go.jp
Hisashi Abe, Department of Wood Properties and Processing, Forestry and Forest Products Research Institute, Matsunosato 1, Tsukuba, Ibaraki 305-8687, Japan, E-mail: abeq@ffpri.affrc.go.jp
Hiroaki Horiyama, Keisuke Kojiro and Yuzo Furuta, Division of Environmental Sciences, Graduate School of Life and Environmental Sciences, Kyoto Prefectural University, Hangi-cho, Shimogamo, Sakyo-ku, Kyoto 606-8522, Japan, E-mail: s821732002@kpu.ac.jp (H. Horiyama), kojiro@kpu.ac.jp (K. Kojiro), furuta@kpu.ac.jp (Y. Furuta)

did not provide any basis for this in their results. Olsson and Salmén (1997) investigated the relationship between the thermal-softening temperature of wood and the lignin content or methoxyl group content, which was calculated as a molar percentage of the methoxyl groups per phenylpropane unit of lignin. They showed a correlation between thermal-softening temperature and the methoxyl group content. Furuta et al. (2010) measured the thermal-softening properties of delignified wood. They clarified that the thermal-softening temperature of water-saturated wood in the lateral direction varied widely under the influence of a slight change in the lignin structure, rather than a reduction in the amount of lignin. The above researches indicate that there is a main relation between the diversity in thermal-softening properties and lignin structure. However, the reasonable grounds for wood why the diverse thermal-softening properties are expressed cannot be discussed.

Wu et al. (1992) investigated the lignin structure of hardwood using ultraviolet and visible microspectrophotometry, and clarified that the distributions of the syringyl and guaiacyl units of lignin in the vessel and fiber differed according to the habitat and porosity of the wood. According to the classification by Wu et al. (1992), the wood species in sub-frigid zones are rich in syringyl units, while those in tropical zones are rich in guaiacyl units. Therefore, the diversity of thermal-softening temperatures may be related to the lignin structure classified according to the climatic zone of the trees. If such a relationship exists between the physical properties and chemical structure of wood and its growing environment, an understanding of tree evolution and growth strategies can be developed.

In addition, the thermal-softening properties of water-swollen wood are affected by the drying history and cooling rate before measurement, even in the same sample (Furuta et al. 2001, 2008a, b; Kojiro et al. 2008). Moreover, the thermal-softening properties of samples collected from a certain part of a tree with large amounts of extractives, such as the base of the branch can be altered by removing the extractives (Furuta et al. 2014). Therefore, to comprehensively discuss the factors affecting the thermal-softening temperatures of various wood species, it is necessary to conduct experiments that consider the thermal history and extraction treatment of the samples before measurement.

In this study, the thermal-softening properties of various wood specimens, registered in the xylarium of the Forestry and Forest Products Research Institute (TWTw), were measured to reveal the diversity of thermal-softening properties and identify the factors that determine the thermal-softening temperature. Dynamic viscoelastic analysis (DMA) was conducted on specimens subjected to the same heating-cooling history, both with and without extraction treatment, to obtain the precise thermal-softening properties in water-saturated conditions. Since the thermal-softening properties in lateral direction are affected by the density and anatomic features of the wood, the correlation between the thermal-softening property and the density and vessel arrangement type of the wood was investigated. In addition, to clarify the factors that determine the diversity in thermal-softening temperature, the syringyl ratio of lignin (syringyl/(syringyl+guaiacyl)) was measured in the samples used for DMA measurement, and the relationship between thermal-softening temperature and lignin structure was investigated. Elucidating the factors contributing to the diversity of the thermal-softening properties of wood is valuable for basic research and for facilitating advanced discussions on the mechanisms of thermal-softening properties.

2 Materials and methods

2.1 Pretreatment of samples

A total of 15 softwood and 72 hardwood specimens were obtained from the xylarium of the Forestry and Forest Products Research Institute (TWTw). The annual rainfall data were obtained from the Japan Meteorological Agency (https://www.data.jma.go.jp/gmd/risk/obsdl/) and the World Weather Online (https://www.worldweatheronline.com/), based on the registered latitude and longitude information. For specimens without latitude information, the latitude data was estimated from the name of the registered region or representative point in the country (Table 1).

For DMA measurement, each wood sample was cut in the longitudinal direction into an end-grain plate (1 mm thickness). Subsequently, the strip-shaped DMA samples (3.2 mm (tangential) × 30 mm (radial)) and square-shaped weight measurement samples (15 mm (tangential) × 15 mm (radial)) were cut from the plate (Figure 1). Half of the DMA samples were extracted for 6 h with ethanol:benzene (1:2, v/v) in a Soxhlet extractor to remove the resin, fat, wax, and soluble tannin. The extracted DMA samples were air-dried at room temperature and freeze-dried for 6 h to completely volatilize the liquid. The weight measurement samples were first treated in the same manner as the extracted DMA samples. Next, they were boiled for 10 min and cooled naturally to room temperature in water. This process was performed two times according to the temperature rise and fall program of the DMA samples. The weight loss rate due to the extraction treatment was calculated by weighing the oven-dried (105 °C) samples (Figure 2). The density of all the samples was obtained from the dimensions and weight of the oven-dried weight measurement samples before extraction. The weight loss due to extraction and density were calculated from the average value measured from two or three weight measurement samples that could be taken from each specimen.

2.2 Dynamic viscoelasticity measurement

A forced-vibration dynamic viscoelastometer (DMA 42E-SF 28 Artemis, NETZSCH Japan K.K., Kanagawa, Japan) was used to measure the

Table 1: List of examined wood species. The syringyl ratio and peak temperature of tan δ were measured for water-saturated, untreated specimens in radial direction. Codes in Köppen climate classification (Kottek et al. 2006); tropical rainforest climate (Af); tropical savanna, wet (Aw); humid subtropical climate (Cfa); hot-summer humid continental climate (Dfa); and warm-summer humid continental climate (Dfb). The specimen with TWTw ID 12075 was classified as Af because it is a tropical wood species lacking provenance.

Scientific name	TWTw sample ID	Vessel arrangement type	Provenance	Köppen climate classification	Latitude (°)	Annual rainfall (mm)	Density (kg/m^3)	Total extraction (%)	Syringyl ratio	Untreated sample		Extracted sample	
										Peak temperature of tan δ (°C)	tan δ value of peak temperature (°C)	Peak temperature of tan δ (°C)	tan δ value of peak temperature (°C)
Quercus gilva	21463	Radial-porous	Taiwan	Cfa	23.9	2323	890	4.2	0.56	77	0.15	78	0.15
Quercus gilva	1017	Radial-porous	Taiwan	Cfa	23.9	2323	920	7.2	0.65	70	0.17	70	0.17
Quercus gilva	1031	Radial-porous	Taiwan	Cfa	23.9	2323	930	4.0	0.77	78	0.12	72	0.15
Quercus gilva	14447	Radial-porous	Chiba, Japan	Cfa	35.2	2047	900	3.1	0.56	80	0.14	80	0.14
Quercus gilva	9317	Radial-porous	Miyazaki, Japan	Cfa	31.9	2626	800	6.1	0.59	78	0.15	80	0.15
Quercus gilva	17750	Radial-porous	Miyazaki, Japan	Cfa	32.0	2774	760	4.8	0.68	75	0.13	76	0.14
Quercus morii	1055	Radial-porous	Taiwan	Cfa	23.9	2323	910	4.5	0.66	71	0.14	71	0.14
Quercus morii	1018	Radial-porous	Taiwan	Cfa	23.6	2323	910	6.9	0.57	72	0.16	73	0.16
Quercus morii	21465	Radial-porous	Taiwan	Cfa	23.9	2323	920	7.2	0.63	72	0.15	73	0.15
Quercus longinux	21464	Radial-porous	Taiwan	Cfa	23.9	2323	1020	5.3	0.59	76	0.16	77	0.15
Quercus pseudomolucea	8194	Radial-porous	Indonesia	Af	−7.7	3420	830	10.7	0.53	72	0.15	72	0.14
Quercus gamelliflora	10018	Radial-porous	Malaysia	Af	5.9	3296	870	3.0	0.70	78	0.11	77	0.12
Quercus acuta	23641	Radial-porous	Gifu, Japan	Cfa	35.2	1964	910	7.5	0.74	77	0.14	74	0.13
Quercus glaber	18790	Radial-porous	Miyazaki, Japan	Cfa	31.9	2774	880	11.3	0.58	75	0.12	72	0.13
Quercus crispula	23715	Ring-porous	Mie, Japan	Cfa	34.2	2158	820	3.3	0.73	71	0.12	72	0.12
Quercus crispula	16810	Ring-porous	Russia	Dfa	46.8	884	780	5.2	0.65	74	0.11	74	0.12
Quercus crispula	27253	Ring-porous	Oita, Japan	Cfa	32.8	2405	720	7.5	0.66	75	0.11	75	0.12
Quercus crispula	25002	Ring-porous	Hokkaido, Japan	Dfa	42.0	1075	700	6.8	0.69	74	0.11	75	0.11
Quercus crispula	21861	Ring-porous	Hokkaido, Japan	Dfa	43.1	1146	660	7.6	0.72	73	0.12	73	0.12
Quercus crispula	970	Ring-porous	Hokkaido, Japan	Dfa	43.1	1146	480	5.4	0.69	70	0.14	72	0.12
Lithocarpus soleriana	5056	Radial-porous	Philippines	Af	14.6	2326	900	6.4	0.51	79	0.14	79	0.15
Lithocarpus edulis	19332	Radial-porous	Okinawa, Japan	Cfa	26.8	2594	730	4.2	0.55	74	0.14	73	0.15

Table 1: (continued)

Scientific name	TWTw sample ID	Vessel arrangement type	Provenance	Köppen climate classification	Latitude (°)	Annual rainfall (mm)	Density (kg/m^3)	Total extraction (%)	Syringyl ratio	Untreated sample		Extracted sample	
										Peak temperature of tan δ (°C)	tan δ value of peak temperature (°C)	Peak temperature of tan δ (°C)	tan δ value of peak temperature (°C)
Lithocarpus edulis	861	Radial-porous	Kagoshima, Japan	Cfa	31.4	2686	830	4.6	0.37	78	0.12	76	0.13
Lithocarpus edulis	26568	Radial-porous	Ibaraki, Japan	Cfa	36	1326	770	5.6	0.6	79	0.14	80	0.14
Lithocarpus clementiana	10025	Radial-porous	Malaysia	Af	5.9	3296	910	4.5	0.62	81	0.12	80	0.13
Lithocarpus glaber	25560	Radial-porous	Kumamoto, Japan	Cfa	32.3	2535	620	5.5	0.57	81	0.12	80	0.13
Acer carpinifolium	23668	Diffuse-porous	Gifu, Japan	Cfa	35.3	1964	670	1.4	0.16	84	0.11	86	0.11
Acer carpinifolium	18574	Diffuse-porous	Yamanashi, Japan	Cfa	35.8	1213	620	2.7	0.47	79	0.12	80	0.12
Acer carpinifolium	24219	Diffuse-porous	Nagano, Japan	Cfa	35.8	2110	660	2.0	0.09	82	0.11	85	0.11
Acer mono	975	Diffuse-porous	Hokkaido, Japan	Dfa	43.4	1146	710	5.5	0.7	72	0.13	75	0.14
Acer mono	14440	Diffuse-porous	Tokyo, Japan	Cfa	35.6	1643	740	3.2	0.64	73	0.12	76	0.12
Acer mono	7418	Diffuse-porous	China	Dfa	39.9	531	680	6.1	0.64	73	0.12	73	0.12
Gardenia jasminoides	12919	Diffuse-porous	Okinawa, Japan	Cfa	26.8	2594	870	7.3	0.69	80	0.12	79	0.12
Gardenia jasminoides	17459	Diffuse-porous	Okinawa, Japan	Cfa	24.3	2025	820	10.5	0.65	79	0.11	81	0.12
Gardenia jasminoides	19484	Diffuse-porous	Kagoshima, Japan	Cfa	28.2	2375	830	9.4	0.65	80	0.11	80	0.12
Distylium racemosum	27840	Diffuse-porous	Fukuoka, Japan	Cfa	33.8	1665	930	5.8	0.53	79	0.11	80	0.12
Distylium racemosum	25950	Diffuse-porous	Tokyo, Japan	Cfa	35.7	1598	740	2.5	0.71	78	0.10	78	0.10
Distylium racemosum	19673	Diffuse-porous	Nagasaki, Japan	Cfa	34.5	1435	920	4.6	0.51	76	0.12	79	0.12
Cercidiphyllum japonicum	4339	Diffuse-porous	Saitama, Japan	Cfa	35.9	1375	570	4.5	0.55	77	0.13	77	0.13
Cercidiphyllum japonicum	9328	Diffuse-porous	Hokkaido, Japan	Dfa	42.9	1061	440	4.8	0.5	78	0.13	80	0.13
Cercidiphyllum japonicum	28908	Diffuse-porous	Ibaraki, Japan	Cfa	36.0	1326	550	4.9	0.46	78	0.11	79	0.11

Table 1: (continued)

Scientific name	TWTw sample ID	Vessel arrangement type	Provenance	Köppen climate classification	Latitude (°)	Annual rainfall (mm)	Density (kg/m^3)	Total extraction (%)	Syringyl ratio	Untreated sample		Extracted sample	
										Peak temperature of tan δ (°C)	tan δ value of peak temperature (°C)	Peak temperature of tan δ (°C)	tan δ value of peak temperature (°C)
Populus maximowiczii	12370	Diffuse-porous	Kyoto, Japan	Cfa	35.3	1808	370	4.9	0.58	78	0.13	78	0.12
Populus maximowiczii	9297	Diffuse-porous	Hokkaido, Japan	Dfb	43.1	920	380	4.3	0.45	80	0.13	80	0.13
Populus maximowiczii	13681	Diffuse-porous	Hokkaido, Japan	Dfb	42.6	1239	420	5.0	0.54	78	0.14	79	0.13
Hebe salicifolia	–	Diffuse-porous	New Zealand	Cfa	−42.4	710	640	5.7	0.74	73	0.13	73	0.12
Ceiba pentandra	7169	Diffuse-porous	Mexico	Cfa	19.4	1003	420	8.7	0.59	77	0.11	76	0.11
Ceiba pentandra	5504	Diffuse-porous	Mexico	Cfa	19.4	1003	190	18.8	0.69	76	0.11	74	0.11
Ceiba pentandra	5612	Diffuse-porous	Nigeria	Cfa	9.6	1216	350	13.6	0.67	71	0.12	74	0.12
Falcataria moluccana	12075	Diffuse-porous	–	Af	–	–	240	3.3	0.63	78	0.10	80	0.09
Falcataria moluccana	11400	Diffuse-porous	New Britain, Papua New Guinea	Af	−9.4	1183	490	3.3	0.58	76	0.13	76	0.13
Falcataria moluccana	11509	Diffuse-porous	Indonesia	Af	−6.1	1907	410	3.8	0.63	80	0.13	79	0.13
Shorea parvistipulata	12929	Diffuse-porous	Malaysia	Af	3.1	2842	510	5.4	0.42	87	0.14	86	0.14
Shorea leprosula	25109	Diffuse-porous	Borneo, Indonesia	Af	−1.0	3151	730	3.1	0.28	89	0.12	89	0.12
Shorea pauciflora	19978	Diffuse-porous	Malaysia	Af	3.1	2842	580	3.8	0.34	91	0.14	92	0.14
Eusideroxylon zwageri	3150	Diffuse-porous	Indonesia	Af	−6.1	1907	1040	4.7	0.1	89	0.18	91	0.17
Eusideroxylon zwageri	13083	Diffuse-porous	Borneo, Indonesia	Af	−1.0	3151	1040	3.5	0.04	90	0.25	93	0.25
Eusideroxylon zwageri	12070	Diffuse-porous	Borneo, Indonesia	Af	−1.0	3151	1090	4.9	−0.14	85	0.25	88	0.25
Fraxinus mandshurica	9344	Ring-porous	Hokkaido, Japan	Dfb	42.9	1061	660	4.2	0.59	75	0.12	75	0.12
Fraxinus mandshurica	21867	Ring-porous	Hokkaido, Japan	Dfb	43.1	1146	680	3.3	0.62	77	0.10	77	0.11
Fraxinus mandshurica	2773	Ring-porous	China	Dfb	39.9	531	620	3.5	0.6	72	0.11	76	0.11
Zelkova serrata	18339	Ring-porous	Ibaraki, Japan	Cfa	36.0	1326	690	10.1	0.67	77	0.12	73	0.12

Table 1: (continued)

Scientific name	TWTw sample ID	Vessel arrangement type	Provenance	Köppen climate classification	Latitude (°)	Annual rainfall (mm)	Density (kg/m^3)	Total extraction (%)	Syringyl ratio	Untreated sample		Extracted sample	
										Peak temperature of tan δ (°C)	tan δ value of peak temperature (°C)	Peak temperature of tan δ (°C)	tan δ value of peak temperature (°C)
Zelkova serrata	13676	Ring-porous	Tokyo, Japan	Cfa	35.7	1643	740	12.2	0.57	74	0.13	73	0.13
Zelkova serrata	9326	Ring-porous	Gunma, Japan	Cfa	36.1	1250	620	10.6	0.55	73	0.13	74	0.12
Tetracentron sinense	13657	Non-porous	China	Aw	39.9	531	380	3.5	0.57	74	0.16	74	0.15
Tetracentron sinense	7486	Non-porous	China	Aw	39.9	531	410	4.0	0.58	75	0.17	72	0.17
Tetracentron sinense	7808	Non-porous	British	Aw	51.5	633	450	6.1	0.57	73	0.15	74	0.13
Trochodendron aralioides	2842	Non-porous	Kyoto, Japan	Cfa	35.1	1523	540	2.5	0.7	72	0.15	71	0.14
Trochodendron aralioides	855	Non-porous	Kumamoto, Japan	Cfa	32.3	2497	670	4.3	0.64	71	0.17	70	0.16
Trochodendron aralioides	14727	Non-porous	Tokyo, Japan	Cfa	35.7	1643	680	1.6	0.65	71	0.16	71	0.16
Gnetum gnemon	6580	Diffuse-porous	Philippines	Af	14.6	2326	650	4.5	0.64	76	0.15	72	0.15
Gnetum gnemon	22089	Diffuse-porous	Java, Indonesia	Af	−7.7	3420	720	3.1	0.57	84	0.10	83	0.10
Gnetum gnemon	13738	Diffuse-porous	Malaysia	Af	3.1	2842	700	2.7	0.66	79	0.12	76	0.11
Ginkgo biloba	28959	Softwood	Ibaraki, Japan	Cfa	36.0	1326	470	2.1	−0.04	93	0.12	94	0.13
Ginkgo biloba	79	Softwood	Tokyo, Japan	Cfa	35.7	1643	540	7.3	0.01	88	0.15	94	0.14
Ginkgo biloba	21789	Softwood	Hokkaido, Japan	Dfa	43.1	1146	570	6.7	0.07	86	0.14	92	0.13
Cryptomeria japonica	9290	Softwood	Akita, Japan	Cfa	39.7	2053	340	4.2	0.04	93	0.13	95+	0.14+
Cryptomeria japonica	6427	Softwood	Tokyo, Japan	Cfa	35.7	1643	370	4.5	−0.12	95+	0.13+	95+	0.13+
Cryptomeria japonica	12854	Softwood	Okinawa, Japan	Cfa	26.8	2594	640	4.7	−0.05	91	0.15	95+	0.14+
Chamaecyparis obtusa	28890	Softwood	Ibaraki, Japan	Cfa	36.1	1326	410	8.8	−0.03	91	0.12	95+	0.13+
Chamaecyparis obtusa	9293	Softwood	Nagano, Japan	Cfa	35.8	1927	390	5.7	0.03	91	0.15	95+	0.15+
Chamaecyparis obtusa	14666	Softwood	Tokyo, Japan	Cfa	35.7	1643	380	6.6	−0.12	92	0.14	95+	0.16+

Table 1: (continued)

Scientific name	TWTw sample ID	Vessel arrangement type	Provenance	Köppen climate classification	Latitude (°)	Annual rainfall (mm)	Density (kg/m^3)	Total extraction (%)	Syringyl ratio	Untreated sample		Extracted sample	
										Peak temperature of tan δ (°C)	tan δ value of peak temperature (°C)	Peak temperature of tan δ (°C)	tan δ value of peak temperature (°C)
Larix kaempferi	16334	Softwood	Ibaraki, Japan	Cfa	36.3	1368	790	14.8	−0.06	93	0.14	93	0.14
Larix kaempferi	9279	Softwood	Nagano, Japan	Cfa	36.2	964	520	12.4	−0.05	95+	0.15+	95+	0.16+
Larix kaempferi	8887	Softwood	Netherlands	Dfb	52.1	853	610	15.8	0.03	91	0.14	94	0.14
Agathis borneensis	17742	Softwood	Malaysia	Af	3.1	2842	480	2.3	−0.08	93	0.17	92	0.16
Agathis borneensis	20089	Softwood	Malaysia	Af	3.1	2842	470	1.3	0.07	90	0.15	89	0.14
Agathis borneensis	3103	Softwood	Indonesia	Af	−6.1	1907	450	7.2	0.06	91	0.15	93	0.15

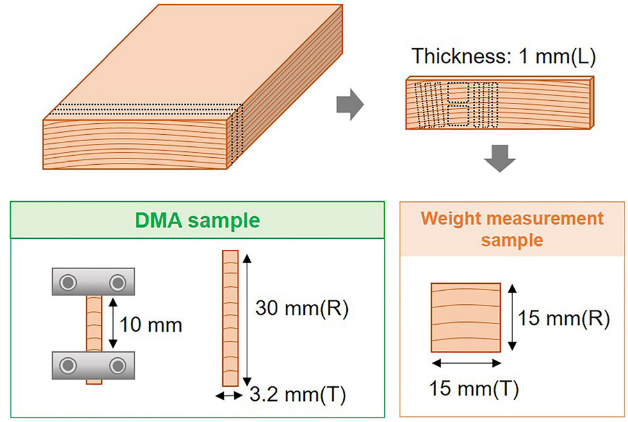

Figure 1: Sample dimensions used for measurements.

temperature-dependent, dynamic viscoelastic properties of the unextracted and extracted water-swollen samples. The dynamic viscoelastic properties of wood changed due to the drying history or cooling rate, even for the same samples (Furuta et al. 2001, 2008a, b; Kojiro et al. 2008). Therefore, to unify the heating history immediately before viscoelastic measurement for all the specimens, this study recorded the data in the second temperature rise after cooling them from 95 °C to 5 °C at 1 °C/min (Figure 2). The data for temperatures up to 98 °C were obtained originally, which is very close to the boiling point of water. Since some samples contained noise in the temperature range higher than 95 °C, DMA data up to 95 °C, which could be stably measured, was analyzed to compare the results. During the viscoelastic measurement, the span was 10 mm in radial direction (Figure 1) and a 0.1 Hz sine wave with a tension displacement amplitude of 5 µm was applied to the sample. In the preliminary experiments conducted on several wood samples, the offset loads in the measured temperature range, when the displacement amplitude was controlled at 5 µm, were within the linear region of the stress-strain line. DMA measurement was performed one time for each sample because the preliminary experiments confirmed that the same temperature program would produce nearly identical measurement results. As an example of the measured DMA data, the results of the temperature dependence of tan δ before and after extraction for softwood and hardwood samples are shown in Figure 3. The peak top of tan δ was read as the peak temperature.

2.3 Estimation of the syringyl ratio

The extracted DMA samples, which were used for the dynamic viscoelastic measurements, were analyzed using an IR spectrometer (FT/IR-4700, JASCO Corporation, Tokyo, Japan). Fine wood meal was prepared from the middle length portion of dried DMA samples, using a glass file, mixed at 1 % with KBr and pressed into a disc. Each spectrum was based on 64 scans with a wavenumber range from 4000 to 500 cm^{-1}. Following Huang et al. (2012), the areas under the IR peak at 1595 cm^{-1} (range: 1605–1574 cm^{-1}, A_{1595}) and 1509 cm^{-1} (range: 1535–1492 cm^{-1}, A_{1509}) were measured. Huang et al. (2012) presented a linear regression equation with a correlation coefficient of 0.98 to describe the relationship between the syringyl ratio (syringyl/(syringyl+guaiacyl)) of lignin aromatics, measured by alkaline nitrobenzene oxidation analysis, and log (peak area ratio of A_{1595}/A_{1509}). In the present study, the same regression equation was used to determine the syringyl ratio of all the

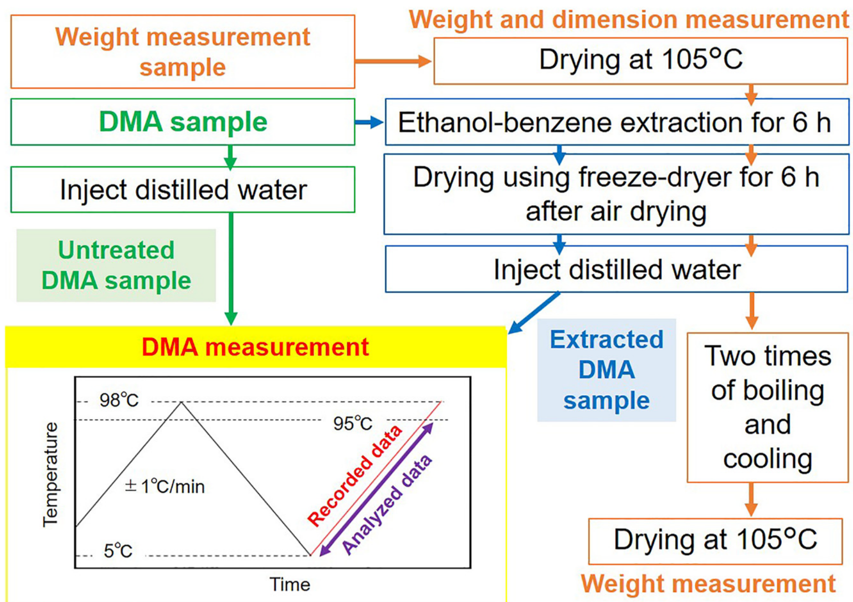

Figure 2: Sample preparation procedures and temperature program for dynamic viscoelastic measurement.

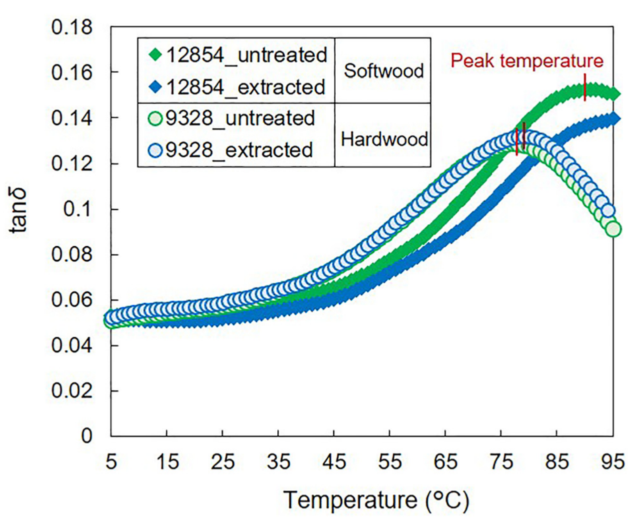

Figure 3: Examples of DMA data for untreated and extracted samples.

specimens from their IR spectra. The peak areas were measured three times for each sample, and after confirming that there were no outliers, area ratios were calculated from the data that showed the clearest spectrum with the least noise.

3 Results and discussion

3.1 Relationship between thermal-softening temperature and the growing environment of the wood

In this study, the peak temperature of tan δ is defined as the thermal-softening temperature of the sample. In this paper, the peak temperatures of tan δ were read for samples for which the peak was observed in the range of 95 °C. Samples for which no peak was observed at 95 °C are indicated as 95+ in Table 1, and the legend is marked in red in the figure. The tan δ values for the 95+ samples were read at 95 °C and indicated in Table 1. Figure 4 shows the relationship between the peak temperature of and the value of tan δ. The peak temperatures of tan δ were slightly different between the extracted and unextracted samples (Figure 4a and b, respectively). Six softwood samples were identified in which the extraction process changed the peak temperature to 95 °C or higher. Table 1 shows that the peak temperature of tan δ in softwoods changed to higher temperatures after extraction. However, some hardwood samples showed a decrease in the peak temperature of tan δ due to extraction. Although the thermal-softening temperatures changed by a maximum of 6 °C due to extraction, the temperature range and the direction of increase or decrease varied among individual samples. No uniform trend was observed among the wood species and no correlation was observed between the peak temperature and the value of tan δ in Figure 4. The peak temperature of tan δ is generally lower for hardwood and higher for softwood, as reported in previous studies (Furuta et al. 2001, 2008a, b). In hardwood species, the peak temperature of tan δ in the radial-, ring-, and non-porous samples was in a temperature range from 70 to 80 °C; however, the temperature range was wider for diffuse-porous samples. The two diffuse-porous samples (both were Ulin (*Eusideroxylon zwageri*), which is a tropical hardwood) showed higher tan δ values than the others. Table 1 lists the peak temperature of tan δ for unextracted specimens, showing some variation within the same wood species.

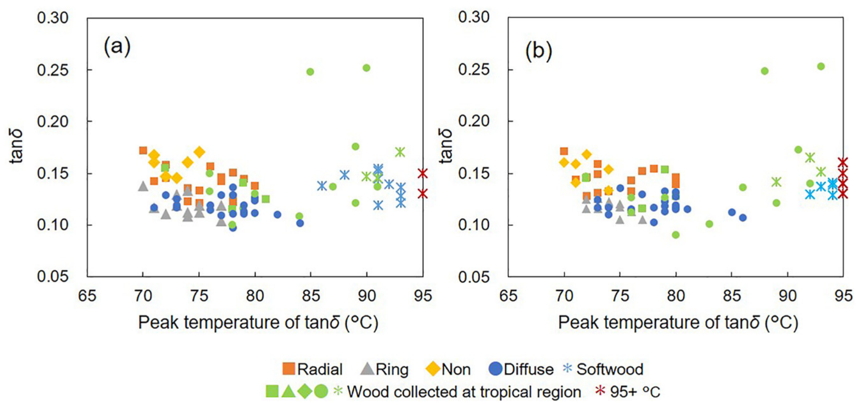

Figure 4: Relationship between loss tangent (tan δ) and peak temperature of tan δ in water-saturated radial samples measured at 0.1 Hz. (a) Untreated samples and (b) extracted samples. The symbol for hardwood species indicates the vessel arrangement type. “Non” = vesselless. Samples collected from tropical climates are presented in green. Samples for which the peak temperature of tan δ could not be observed by 95 °C are presented in red.

Previous studies have reported that among hardwood species, tropical species show higher thermal-softening temperatures (Furuta et al. 2010) and are rich in guaiacyl units (Wu et al. 1992). If both the physical properties and chemical structures observed in tropical wood species are determined by their habitat, the regional climate may exert an influence on the thermal-softening temperature. To confirm this possibility, the relationship between the peak temperature of tan δ in untreated specimens and the latitude and annual rainfall at the collection site is plotted in Figure 5.

The softwood specimens showed high peak temperatures of tan δ, regardless of latitude. Among the hardwood specimens, the radial-porous and diffuse-porous wood cover a wide latitude range. Certain diffuse-porous specimens collected from near the equator exhibited high peak temperatures compared to softwood. This distribution of the peak temperature of tan δ was similar to the high peak temperatures of tan δ previously observed in tropical hardwood species (Furuta et al. 2001, 2008a, b). However, this study suggests that the latitude does not necessarily correspond to the thermal-softening temperature among various wood species.

Specifically, in softwood and hardwood except diffuse-porous wood, no relationship was observed between the annual rainfall and peak temperature of tan δ (Figure 5b). Among the diffuse-porous specimens, there was only a weak positive correlation between the two parameters. However, this correlation could be enhanced in certain tropical diffuse-porous wood, because many areas with high rainfall are located near the equator (see the clustering of diffuse-porous specimens near 0° latitude in Figure 5a). Overall, neither the latitude nor annual precipitation were related to the thermal-softening temperatures of wood in this study.

3.2 Relationship between thermal-softening property and density

In this section, the thermal-softening properties of extracted samples are presented to discuss the relationship between the wood cell wall constituents and the thermal-softening properties. Figure 6a–c plot the storage elastic modulus (E') at 30 °C, loss elastic modulus (E'') at 30 °C, and peak temperatures of tan δ versus the wood density, respectively. A positive correlation was observed between E' and density in softwood, ring-porous hardwood, non-porous hardwood, and diffuse-porous hardwood, all following the same linear relationship. However, radial-porous wood was distributed

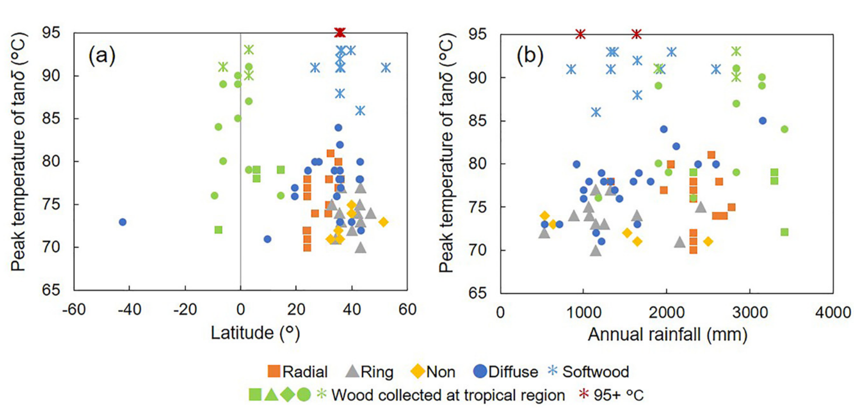

Figure 5: Relationship between habitat and peak temperature of tan δ of water-saturated, untreated radial specimens measured at 0.1 Hz. The symbol for hardwood species indicates the vessel arrangement type. “Non” = vesselless. Samples collected from tropical climates are presented in green. Samples for which the peak temperature of tan δ could not be observed by 95 °C are presented in red.

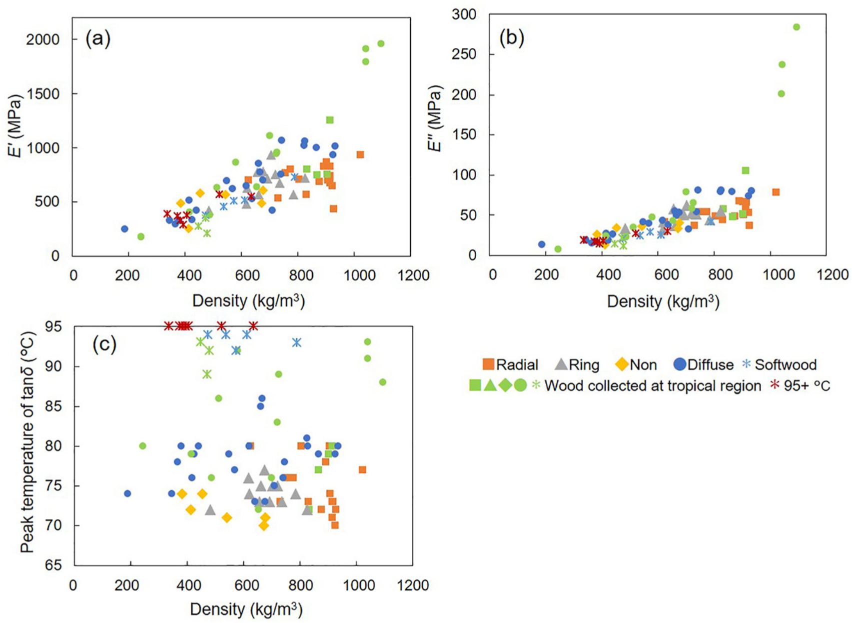

Figure 6: Relationship between data from dynamic viscoelastic measurements at 0.1 Hz and the density of extracted radial specimens in water-saturated conditions. (a) Storage elastic modulus (E') at 30 °C, (b) loss elastic modulus (E'') at 30 °C, and (c) peak temperatures of tan δ. The symbol for hardwood species indicates the vessel arrangement type. "Non" = vesselless. Samples collected from tropical climates are presented in green. Samples for which the peak temperature of tan δ could not be observed by 95 °C are presented in red.

at slightly lower locations and did not display a clear positive correlation with density. The relationship between E'' and density showed a positive correlation when the density was 1000 kg/m^3 or less. The distribution patterns of E'' and E' were nearly the same. Figure 6a and b presents three Ulin specimens with the highest densities (1000 kg/m^3 or more). Their E' and E'' values deviate from the linear distribution of the other specimens. While E' and E'' show a positive correlation with wood density, the peak temperature of tan δ shows no such relationship (Figure 6c). Thus, the wood species exhibited a wide range of thermal-softening temperatures, regardless of their density.

3.3 Relationship between thermal-softening property and lignin structure

To investigate the relationship between thermal-softening temperature and lignin structure, the syringyl ratio of lignin aromatics was estimated from the peak area ratio of the IR spectrum. Since the sample used for the IR measurement had undergone a heating history during DMA measurement, there was a possibility that the syringyl ratio would be slightly different from that of the untreated sample. However, this experiment prioritized the comparison of the results with the same sample.

Understanding the partial structure of lignin is useful for inferring its structural characteristics. The β-O-4 and phenylcoumarin structures are the specific partial structures responsible for lignin's linear chain, while the biphenyl (5-5 bond) and diaryl ether structures (4-O-5 structure) are responsible for its branch chain. The composition ratio of the partial structures changes according to the aromatic nucleus during lignin production. The main reason for this is that the aromatic nuclei of guaiacyl can be coupled at the 5-position to form fused structures, such as β-5, 5-5, and 4-O-5, whereas the aromatic nuclei of syringyl cannot be coupled alone at the 5-position due to the methoxy group, which acts as the substitute (Stewart et al. 2009). Akiyama et al. (2005) investigated the relationship between the partial structure of lignin and the syringyl ratio of lignin aromatics in various wood species and found that the biphenyl structure content decreased quadratically with an increase in the syringyl ratio. Based on previous research and this study's results, it can be concluded that wood species with a low syringyl ratio have a dense lignin structure, with several condensed structures derived from the guaiacyl unit, whereas wood species with a high syringyl ratio have a sparse lignin structure, with several linear partial structures.

In Figure 7, the syringyl ratio is distributed in a wide range from 0 to 0.8 (approximately), and almost 0 in softwood and tropical hardwood species. Since softwood has no syringyl aromatic nuclei, the syringyl ratio should be exactly 0. However, the syringyl ratio was estimated using a calibration curve with an error of about ±0.2. Tropical hardwood samples showed a wide range of syringyl ratios, indicating that these samples are not necessarily rich in the guaiacyl unit. Nevertheless, several samples showed particularly low syringyl ratios. Hardwoods with syringyl ratios near 0 possessed a high peak temperature of tan δ compared to softwoods. Thus, the syringyl ratio and peak temperature of tan δ display a negative correlation. Based

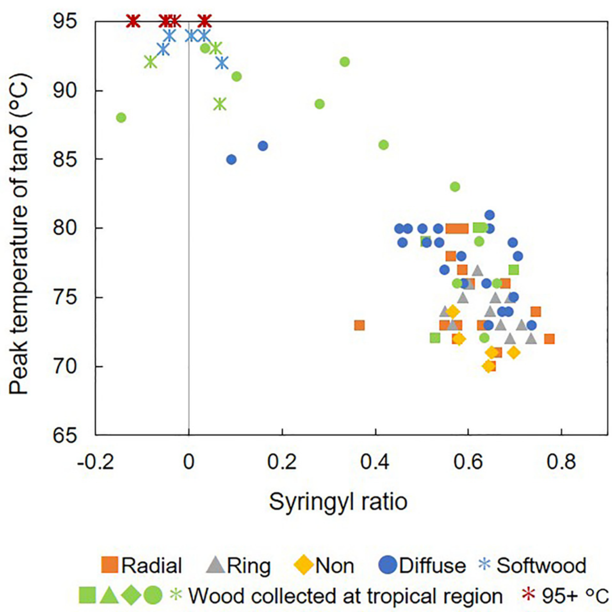

Figure 7: Relationship between peak temperature of tan δ measured at 0.1 Hz and syringyl ratio of extracted radial specimens. The symbol for hardwood species indicates the vessel arrangement type. "Non" = vesselless. Samples collected from tropical climates are presented in green. Samples for which the peak temperature of tan δ could not be observed by 95 °C are presented in red.

on the interpretation of the partial structure of lignin, the peak temperature of tan δ is considered to be higher for wood species with denser lignin structures and lower for those with sparser lignin structures. It is known that in polymers, the glass transition temperature (T_g) shifts to higher values as the crosslink density increases (Nielsen 1962). In wood, the peak temperature of tan δ, derived from lignin, could similarly depend on the lignin's condensation structure in each wood species. Although this study's results were obtained by using the calibration curves of IR spectra, they supported the correlation shown by Olson and Salmén (1997) between thermal-softening temperature and methoxyl group content.

4 Conclusions

To elucidate the diversity of the thermal-softening properties of wood, the peak temperature of tan δ was measured for 87 wood specimens from the global collection of the xylarium of Forestry and Forest Products Research Institute. The peak temperature of tan δ was found to be higher for softwood and tropical hardwood species as compared to other hardwood species, regardless of the extraction treatment. There was no clear relationship between the peak temperature of tan δ and the latitude and annual rainfall of the habitat. Furthermore, the peak temperature of tan δ was not uniquely determined by anatomical features and wood species. E' and E'' showed strong correlations with density, regardless of species; however, there was no relationship between the peak temperature of tan δ and density. Furthermore, a positive correlation was observed between the peak temperature of tan δ and the syringyl ratio, which depends on the amounts of different partial structures in lignin. This result indicates that the thermal-softening temperature is higher for wood species with a denser lignin structure (low syringyl ratio) and lower for species with a sparse lignin structure (high syringyl ratio).

Acknowledgments: The authors express their appreciation of Dr. Takami Saito (Forestry and Forest Product Research Institute, Japan) and Dr. Takuya Akiyama (University of Tokyo, Japan) for providing helpful literature and suggestions.
Research ethics: Not applicable.
Author contributions: YM conducted the experiments and wrote the manuscript, HA selected and provided the wood specimens from the wood library of the Forestry and Forest Products Research Institute, HH and KK participated in result discussions, and YF supervised the work. All the authors approved the final version of the manuscript.
Competing interests: The authors states no conflict of interest.
Research funding: This study was supported by the JSPS KAKENHI (grant number: JP20K15570).
Data availability: The raw data can be obtained on request from the corresponding author.

References

Akiyama, T., Goto, H., Nawai, D.S., Syafii, W., Matsumoto, Y., and Meshitsuka, G. (2005). Erythro/threo ratio of β-O-4-5 structures as an important structural characteristic of lignin. Part 4: variation in the erythro/threo ratio in softwood and hardwood lignins and its relation to syringyl/guaiacyl ratio. *Holzforschung* 59: 276–281.

Becker, H. and Noack, D. (1968). Studies on dynamic torsional viscoelasticity of wood. *Wood Sci. Technol.* 2: 213–230.

Furuta, Y., Soma N., Obata, Y., and Kanayama, K. (2001). Research to make better use of wood as sustainable resource – physical property change of wood to heating and drying histories. In: *Proceedings of the fourth international conference on materials for resources 2001 Akita (ICMR 2001), October 11-13, 2001.* SMERJ, Akita, pp. 260–265.

Furuta, Y., Kojiro, J., Nakatani, T., Nakajima, M., and Ishimaru, Y. (2008a). The dynamic viscoelastic properties of wood in nonequilibrium states. *J. Soc. Mater. Sci. Jpn.* 57: 338–343.

Furuta, Y., Nakajima, M., Nakatani, T., Kojiro, K., and Ishimaru, Y. (2008b). Effects of the lignin on the thermal-softening properties of the water-swollen wood. *J. Soc. Mater. Sci. Jpn.* 57: 344–349.

Furuta, Y., Nakajima, M., Nakanii, E., and Ohkoshi, M. (2010). The effects of lignin and hemicellulose on thermal-softening properties of water-swollen wood. *Mokuzai Gakkaishi* 56: 132–138.

Furuta, Y., Okuyama, T., Kojiro, K., Miyoshi, Y., and Kiryu, T. (2014). Temperature dependence of the dynamic viscoelasticity of bases of Japanese cypress branches and the trunk close to the branches saturated with water. *J. Wood Sci.* 60: 249–254.

Huang, Y., Wang, L., Chao, Y., Nawai, D.S., Akiyama, T., Yokoyama, T., and Matsumoto, Y. (2012). Analysis of lignin aromatic structure in wood based on the IR spectrum. *J. Wood Chem. Technol.* 32: 294–303.

Kojiro, K., Furuta, Y., and Ishimaru, Y. (2008). Influence of histories on dynamic viscoelastic properties and dimensions of water-swollen wood. *J. Wood Sci.* 54: 95–99.

Kottek, M., Griester, J., Beck, C., Rudolf, B., and Rubel, F. (2006). World map of the Köppen-Geiger climate classification updated. *Meteorol. Zeitschrift* 15: 259–263.

Nielsen, L.E. (1962). *Mechanical properties of polymers*. Reinhold Publishing Corp., New York.

Olsson, A.M. and Salmén, L. (1997). The effect of lignin composition on the viscoelastic properties of wood. Nord. *Pulp Paper Res. J.* 12: 140–144.

Placet, V., Passard, J., and Perré, P. (2007). Viscoelastic properties of green wood across the grain measured by harmonic tests in the range 0–95 °C: hardwood vs. softwood and normal wood vs. reaction wood. *Holzforschung* 61: 548–557.

Salmén, L. (1984). Viscoelastic properties of *in situ* lignin under water-saturated conditions. *J. Mater. Sci.* 19: 3090–3096.

Stewart, J.J., Akiyama, T., Chapple, C., Ralph, J., and Mansfield, S.D. (2009). The effects on lignin structure of overexpression of ferulate 5-hydroxylase in hybrid poplar. *Plant Physiol.* 150: 621–635.

Wu, J., Fukazawa, K., and Ohtani, J. (1992). Distribution of syringyl and guaiacyl lignins in hardwoods in relation to habitat and porosity form in wood. *Holzforschung* 46: 181–185.